

The Neutron and the Electron Electric Dipole Moment in $N = 1$ Supergravity Unification

Tarek Ibrahim and Pran Nath

Department of Physics, Northeastern University
Boston, MA 02115, USA

Abstract

An analysis of the neutron EDM and of the electron EDM in minimal $N = 1$ supergravity unification with two CP violating phases is given. For the neutron the analysis includes the complete one loop gluino, chargino, and neutralino exchange diagrams for the electric dipole and the chromoelectric dipole operators, and also the contribution of the purely gluonic dimension six operator. It is shown that there exist significant regions in the six dimensional parameter space of the model where cancellations between the gluino and the chargino exchanges reduce the electric and the chromoelectric contributions, and further cancellations among the electric, the chromoelectric, and the purely gluonic parts lead to a dramatic lowering of the neutron EDM sometimes below the electron EDM value. This phenomenon gives a new mechanism, i.e., that of internal cancellations, for the suppression of the neutron EDM in supersymmetric theories. The cancellation mechanism can significantly reduce the severe fine tuning problem associated with CP violating phases in SUSY and SUGRA unified models.

1 Introduction

Supersymmetric models with softly broken supersymmetry introduce new sources of CP violation which contribute to the neutron and the electron electric dipole moment (EDM). It is known that the exchange of SUSY particles close to their current experimental lower limits and CP violating phases of normal size, i.e. $O(1)$, will lead to the neutron EDM already in excess of the current experimental bound of $1.1 \cdot 10^{-25}$ ecm [1]. Two possibilities to resolve this problem have been commonly discussed in the literature. The first is that the phases are not $O(1)$ but rather much smaller, i.e., $O(10^{-2} - 10^{-3})$ [2, 3, 4]. However, a small phase constitutes a fine tuning unless it arises naturally, e.g. as a loop correction. The second possibility is that the phases are $O(1)$, but the supersymmetric spectrum which contributes to the EDMs is heavy [5, 6], i.e. in the several TeV region and perhaps out of reach of even the LHC. In this paper we discuss a third possibility, i.e., that of internal cancellations among the different components of the neutron EDM. We shall show that such cancellations can dramatically reduce the neutron EDM without either excessive retuning of the phases or pushing the SUSY spectrum in several TeV mass range. One then finds that the neutron and the electron EDMs can satisfy the current experimental bounds [1, 8] with phases not unduly small and a SUSY spectrum which is not unduly heavy at least for low values of $\tan \beta$.

Although there are many analyses of the EDMs in supersymmetric theories most of these [2, 3, 5, 6, 7] are without radiative breaking of the electro-weak symmetry and sometimes neglecting the chargino contribution to the neutron EDM [2, 7]. For the neutron EDM there are two operators other than the electric dipole moment operator, which can contribute to the neutron EDM. One of these is the color dipole operator and the other is the dimension six purely gluonic operator considered by Weinberg [9]. With the exception of the work of ref. [10] most of the previous analyses [2, 3, 6, 7, 11] do not take into account the contribution of the color and of the purely gluonic operators with the presumption that their relative contributions to the neutron EDM is small. However, it was pointed out in ref. [12] that the contributions of the color and of the purely gluonic operators can be comparable to the contribution of the electric dipole operator in a significant region of the minimal supergravity parameter space [12]. Currently there is some confusion in the literature regarding the sign of the gluino exchange term [6, 7]. Further, there is no analysis aside from that of ref. [6] which gives the complete one loop contribution including the gluino, the chargino and the neutralino ex-

changes against which the signs of the relative contributions of the various terms can be checked. Because of the sensitive issue of the cancellation between the gluino and the chargino exchange diagrams crucial to the analysis of this paper, we have redone the full one loop analysis of the EDM with the gluino, the chargino and the neutralino exchanges. We compare our results to those of Ref. [6, 7] in Appendix A. In our analysis we have made the standard assumption of ignoring all the generational mixing of quarks and of squarks.

The outline of the paper is as follows: In Sec. 2 we give the general features of the minimal supergravity unified model and discuss the new CP violating phases it supports. In Sec.3 we give our evaluation of the gluino, the chargino and the neutralino contributions to the electric dipole operator. In Sec.4 we display our evaluation of the chromoelectric and of the purely gluonic operator contributions. Numerical analysis of results and the phenomenon of cancellation among the various components is discussed in Sec.5. Conclusions are given in Sec.6. Diagonalization of the squark and of the chargino mass matrices paying attention to the phases is given in Appendices A and B along with a comparison of our results with those of the previous analyses.

2 N = 1 Supergravity and CP Violating Phases

The analysis of this paper is based on N = 1 supergravity grand unified theory in which supersymmetry is broken spontaneously via gravitational interactions in the hidden sector [13, 14], and the electro-weak symmetry is broken via radiative effects. We assume that the grand unified theory (GUT) group G breaks at the scale M_G to the Standard Model gauge group, and after breaking of supersymmetry the tree effective theory can be characterized by the following symmetry breaking sector at the GUT scale

$$V_{SB}(0) = m_0^2 Z_a Z^a + (m_0 A_0 W^{(3)} + B_0 W^{(2)} + H \text{c.c.}) + \frac{1}{2} m_{\frac{1}{2}} \lambda_i \lambda_i \quad (1)$$

Here $W^{(2)} = \lambda_0 H_1 H_2$, with H_1, H_2 being the two Higgs doublets, $W^{(3)}$ is the superpotential cubic in the fields, m_0 is the universal scalar mass, A_0 is the universal trilinear coupling, B_0 is the universal bilinear coupling, and $m_{\frac{1}{2}}$ is the universal gaugino mass. In general A_0, B_0, λ_0 and $m_{\frac{1}{2}}$ are complex. However, not all the phases are physical. It is possible to remove the phases of $m_0, m_{\frac{1}{2}}$ and make B_0, λ_0 real by redefinition of the fields and by doing R-transformations on them. We are then left with only two independent phases at the GUT scale. One may choose

one of these to be the phase of ϕ_0 (ϕ_0), and the other to be the phase of A_0 (ϕ_{A0}). Using renormalization group evolution one can evolve $V_{SB}(0)$ to low energy and one finds

$$\begin{aligned}
V_{SB} = & m_1^2 \mathbf{H}_1^\dagger \mathbf{H}_1 + m_2^2 \mathbf{H}_2^\dagger \mathbf{H}_2 - [\mathbf{H}_1^\dagger \mathbf{H}_2 + \text{H.c.}] \\
& + M_G^2 [\mathbf{u}_L \mathbf{u}_L + \mathbf{d}_L \mathbf{d}_L] + M_U^2 \mathbf{u}_R \mathbf{u}_R + M_D^2 \mathbf{d}_R \mathbf{d}_R \\
& + M_L^2 [\tilde{\nu}_e \tilde{\nu}_e + \mathbf{e}_L \mathbf{e}_L] + M_E^2 \mathbf{e}_R \mathbf{e}_R \\
& + \frac{g m_0}{2 m_W} \mathbf{H}_1^\dagger \mathbf{H}_2 [\mathbf{e}_R + \frac{m_d A_d}{\cos} \mathbf{d}_R] + \frac{m_u A_u}{\sin} \mathbf{H}_2^\dagger \mathbf{H}_1 [\mathbf{u}_R + \frac{m_u A_u}{\sin} \mathbf{u}_R] + \text{H.c.} \\
& + \frac{1}{2} [\mathfrak{m}_3 \mathbf{g} \mathbf{g} + \mathfrak{m}_2 \mathbf{W}^a \mathbf{W}^a + \mathfrak{m}_1 \mathbf{B} \mathbf{B}] + V_{SB}
\end{aligned} \tag{2}$$

where $(\mathbf{u}_L, \mathbf{d}_L)$ are the SU(2) (slepton, squark) doublets (the generation indices are suppressed), and V_{SB} is the one loop contribution to the effective potential[15].

In our analysis the electroweak symmetry is broken by radiative effects which allows one to determine the magnitude of ϕ_0 by fixing M_Z and to find the magnitude of B_0 in terms of $\tan \beta = \frac{H_2}{H_1}$. In the analysis we use one-loop renormalization group equations (RGEs) for the evolution of the soft SUSY breaking parameters and for the parameter μ , and two-loop RGEs for the gauge and Yukawa couplings. The equations for the gauge and the Yukawa couplings, and the diagonal elements of the sfermion masses and gaugino masses are such that they are entirely real, while the phase of μ doesn't run because it cancels out of the one loop renormalization group equation of μ . However, both the magnitudes and the phases of A_i do evolve and one has

$$\frac{dA_t}{dt} = \left(\frac{16}{3} \tilde{\alpha}_3 \frac{\mathfrak{m}_3}{m_0} + 3 \tilde{\alpha}_2 \frac{\mathfrak{m}_2}{m_0} + \frac{13}{15} \tilde{\alpha}_1 \frac{\mathfrak{m}_1}{m_0} + 6Y^t A_t + Y^b A_b \right); \tag{3}$$

$$\frac{dA_b}{dt} = \left(\frac{16}{3} \tilde{\alpha}_3 \frac{\mathfrak{m}_3}{m_0} + 3 \tilde{\alpha}_2 \frac{\mathfrak{m}_2}{m_0} + \frac{7}{15} \tilde{\alpha}_1 \frac{\mathfrak{m}_1}{m_0} + Y^t A_t + 6Y^b A_b + Y^A A \right); \tag{4}$$

$$\frac{dA}{dt} = \left(3 \tilde{\alpha}_2 \frac{\mathfrak{m}_2}{m_0} + \frac{9}{5} \tilde{\alpha}_1 \frac{\mathfrak{m}_1}{m_0} + 4Y^A A + 3Y^b A_b \right); \tag{5}$$

$$\frac{dA_u}{dt} = \left(\frac{16}{3} \tilde{\alpha}_3 \frac{\mathfrak{m}_3}{m_0} + 3 \tilde{\alpha}_2 \frac{\mathfrak{m}_2}{m_0} + \frac{13}{15} \tilde{\alpha}_1 \frac{\mathfrak{m}_1}{m_0} + 3Y^t A_t \right); \tag{6}$$

$$\frac{dA_d}{dt} = \left(\frac{16}{3} \tilde{\alpha}_3 \frac{\mathfrak{m}_3}{m_0} + 3 \tilde{\alpha}_2 \frac{\mathfrak{m}_2}{m_0} + \frac{7}{15} \tilde{\alpha}_1 \frac{\mathfrak{m}_1}{m_0} + 3Y^b A_b \right); \tag{7}$$

and

$$\frac{dA_e}{dt} = (3\tilde{\alpha}_2 \frac{m_2}{m_0} + \frac{9}{5} \tilde{\alpha}_1 \frac{m_1}{m_0} + 3Y^b A_b); \quad (8)$$

where $\tilde{\alpha}_i = \frac{g_i^2}{(4\pi)^2}$, $Y_{(u,d,e)} = \frac{h_{(u,d,e)}}{(4\pi)^2}$, and where g_i are the gauge couplings and $h_{(u,d,e)}$ are the Yukawa couplings, and $t = \ln \frac{M_{\text{G}}^2}{Q^2}$. The supergravity model with CP violation is then completely parametrized by just six quantities: $m_0, m_{\frac{1}{2}}, A_0, \tan \beta, \theta$ and α_0 . There are 32 new particles in this model. Their masses and interactions are determined by the six parameters above. Thus the model is very predictive.

3 EDM Calculation

One defines the EDM of a spin- $\frac{1}{2}$ particle by the effective lagrangian

$$L_I = \frac{i}{2} d_f \bar{\psi} \gamma_5 F \quad (9)$$

which in the non-relativistic limit gives $L_I = d_f \bar{\psi} \gamma_5 \psi$ where ψ is the large component of Dirac field. In renormalizable theories the effective lagrangian (9) is induced at the loop level if the theory contains a source of CP violation at the tree level. For a theory of fermion f interacting with other heavy fermions i 's and heavy scalars k 's with masses m_i, m_k and charges Q_i, Q_k the interaction that contains CP violation in general is given by

$$L_{\text{int}} = \sum_{ik} \bar{f} (K_{ik} \frac{1}{2} \gamma_5 + L_{ik} \frac{1}{2}) \psi_i \phi_k + \text{H.c.} \quad (10)$$

Here L violates CP invariance if $\text{Im}(K_{ik} L_{ik}) \neq 0$. The one loop EDM of the fermion f in this case is given by

$$\sum_{ik} \frac{m_i}{(4\pi)^2 m_k^2} \text{Im}(K_{ik} L_{ik}) (Q_i A(\frac{m_i^2}{m_k^2}) + Q_k B(\frac{m_i^2}{m_k^2})) \quad (11)$$

where $A(r)$ and $B(r)$ are defined by

$$A(r) = \frac{1}{2(1-r)^2} (3-r + \frac{2\ln r}{1-r}) \quad (12)$$

and

$$B(r) = \frac{1}{2(r-1)^2} (1+r + \frac{2r\ln r}{1-r}); \quad (13)$$

where one has charge conserved at the vertices, i.e., $Q_k = Q_f - Q_i$. The loop diagrams corresponding to the term A is Fig.(1a) and to the term B is Fig.(1b).

3.1 Gluino Contribution

The quark-squark-gluino interaction is given by [14]:

$$\mathcal{L}_{q\bar{q}g} = \sum_{i=u,d} \bar{q}_i^a T_{jk}^a \gamma^\mu (q_i^j \frac{1}{2} g_s \bar{q}_{iR}^k + q_i^j \frac{1}{2} g_s \bar{q}_{iL}^k) + H.c.; \quad (14)$$

where $a = 1 \dots 8$ are the gluino color indices, and $j,k = 1 \dots 3$ are the quark and squark color indices. The scalar fields \bar{q}_L and \bar{q}_R are in general linear combinations of the mass eigenstates which are given by diagonalizing the squark mass² matrices for u and d at the electroweak scale [14]:

$$M_{\tilde{u}}^2 = \begin{pmatrix} M_{\tilde{Q}}^2 + m_u^2 + M_Z^2 (\frac{1}{2} - Q_u \sin^2 \theta_W) \cos 2\beta & m_u (A_u m_0 - \cot \beta) \\ m_u (A_u m_0 - \cot \beta) & M_{\tilde{U}}^2 + m_u^2 + M_Z^2 Q_u \sin^2 \theta_W \cos 2\beta \end{pmatrix} \quad (15)$$

and

$$M_{\tilde{d}}^2 = \begin{pmatrix} M_{\tilde{Q}}^2 + m_d^2 - M_Z^2 (\frac{1}{2} + Q_d \sin^2 \theta_W) \cos 2\beta & m_d (A_d m_0 - \tan \beta) \\ m_d (A_d m_0 - \tan \beta) & M_{\tilde{D}}^2 + m_d^2 + M_Z^2 Q_d \sin^2 \theta_W \cos 2\beta \end{pmatrix} \quad (16)$$

where $Q_u = \frac{2}{3}$ and $Q_d = -\frac{1}{3}$. We note that the A_u and A_d are not independent but evolve from the same common A_0 at the GUT scale. Further, β (the phase of μ), ϕ_{A_u} (the phase of A_u), and ϕ_{A_d} (the phase of A_d) are related to just the two phases ϕ_0 and ϕ_{A_0} at the GUT scale by renormalization group evolution. We diagonalize the squark mass matrices so that

$$\bar{q}_L = D_{q11} \bar{q}_1 + D_{q12} \bar{q}_2 \quad (17)$$

$$\bar{q}_R = D_{q21} \bar{q}_1 + D_{q22} \bar{q}_2; \quad (18)$$

where \bar{q}_1 and \bar{q}_2 are the mass eigenstates. A more detailed discussion of the diagonalization is given in Appendix A.

In terms of the mass eigenstates \bar{q}_1 and \bar{q}_2 the gluino contribution is given by

$$\mathcal{L}_{q\text{gluino}}^E = e = \frac{2}{3} \sum_{k=1}^3 \text{Im} \left(\frac{1}{q} \right) \frac{m_g}{M_{\tilde{q}_k}^2} Q_q B \left(\frac{m_g^2}{M_{\tilde{q}_k}^2} \right); \quad (19)$$

where $\frac{1}{q} = D_{q21} D_{q1k}$, $s = \frac{g_s^2}{4}$, m_g is the gluino mass, and e is the positron charge.

3.2 Neutralino Contribution

In order to discuss the neutralino exchange contributions we first exhibit the neutralino mass matrix:

$$M_0 = \begin{pmatrix} 0 & m_1 & 0 & M_Z \sin \theta_W \cos \theta_A & M_Z \sin \theta_W \sin \theta_A \\ m_1^* & 0 & m_2 & M_Z \cos \theta_W \cos \theta_A & M_Z \cos \theta_W \sin \theta_A \\ 0 & M_Z \sin \theta_W \cos \theta_A & M_Z \cos \theta_W \cos \theta_A & 0 & 0 \\ M_Z \sin \theta_W \sin \theta_A & M_Z \cos \theta_W \sin \theta_A & 0 & 0 & 0 \end{pmatrix} : \quad (20)$$

The matrix M_0 is a complex non hermitian and symmetric matrix, which can be diagonalized using a unitary matrix X such that

$$X^T M_0 X = \text{diag}(m_0^1; m_0^2; m_0^3; m_0^4) : \quad (21)$$

By rearranging the fermion-fermion-neutralino interaction [12], the neutralino exchange contribution to the fermion EDM is given by

$$d_{f \text{ neutralino}}^E = e = \frac{e M}{4 \sin^2 \theta_W} \sum_{k=1}^2 \sum_{i=1}^4 X^2 X^4 \text{Im} \left(\frac{m_0^i}{M_{fk}^2} Q_f B \left(\frac{m_0^2}{M_{fk}^2} \right) \right); \quad (22)$$

where

$$f_{ik} = \left[\frac{p}{2} \tan \theta_W (Q_f - T_{3f}) X_{1i} + T_{3f} X_{2i} g D_{f1k} + \frac{p}{2} \tan \theta_W Q_f X_{1i} D_{f2k} + \frac{p}{2} \tan \theta_W Q_f X_{1i} D_{f2k} - \frac{p}{2} \tan \theta_W Q_f X_{1i} D_{f2k} \right] : \quad (23)$$

Here we have

$$u = \frac{m_u}{2m_W \sin \theta_W}; \quad d_e = \frac{m_{d,e}}{2m_W \cos \theta_W} \quad (24)$$

where $b = 3(4)$ for $T_{3f} = \frac{1}{2}(\frac{1}{2})$.

3.3 Chargino Contribution

To discuss the contribution of the chargino exchanges we exhibit first the chargino mass matrix

$$M_C = \begin{pmatrix} m_2 & p \frac{m_2}{2m_W \sin \theta_W} \\ p \frac{m_2}{2m_W \cos \theta_W} & 0 \end{pmatrix} \quad (25)$$

This matrix can be diagonalized by the biunitary transformation

$$U M_C V^{-1} = \text{diag}(m_+^1; m_+^2) \quad (26)$$

where U and V are unitary matrices (see Appendix B). By looking at the fermion-fermion-chargino interaction we find the chargino contribution to the EDMs for the up quark, the down quark and for the electron as follows

$$d_{u \text{ chargino}}^E = e = \frac{e M}{4 \sin^2 \theta_W} \sum_{k=1}^2 \sum_{i=1}^2 X^2 X^2 \text{Im} \left(\frac{m_+^i}{M_{dk}^2} Q_d B \left(\frac{m_+^2}{M_{dk}^2} \right) + (Q_u - Q_d) A \left(\frac{m_+^2}{M_{dk}^2} \right) \right); \quad (27)$$

$$d_{\text{d chargino}}^E = e = \frac{e M}{4 \sin^2 \theta_W} \sum_{k=1}^2 \sum_{i=1}^2 \text{Im} \left(\frac{m_{\tilde{d}k}^2}{M_{\tilde{u}k}^2} \right) Q_{\tilde{u}k} B \left(\frac{m_{\tilde{d}k}^2}{M_{\tilde{u}k}^2} \right) + (Q_{\tilde{d}} - Q_{\tilde{u}}) A \left(\frac{m_{\tilde{d}k}^2}{M_{\tilde{u}k}^2} \right); \quad (28)$$

and

$$d_{\text{e chargino}}^E = e = \frac{e M}{4 \sin^2 \theta_W} \frac{m_e}{m_{\tilde{e}}} \sum_{i=1}^2 \text{Im} (U_{i2} V_{i1}) A \left(\frac{m_{\tilde{e}}^2}{m_{\tilde{e}}^2} \right) \quad (29)$$

where

$$u_{ik} = (u_{i2} V_{i1} D_{d1k} - U_{i1} D_{d1k} - u_{i2} V_{i2} D_{d2k}) \quad (30)$$

$$d_{ik} = (d_{i2} U_{i1} D_{u1k} - V_{i1} D_{u1k} - d_{i2} U_{i2} D_{u2k}); \quad (31)$$

The sum total of the gluino, the neutralino and the chargino contributions to the EDM gives us the total EDM. To obtain the neutron EDM contribution from the electric dipole moment operator we use the non-relativistic SU(6) quark model which gives

$$d_n = \frac{1}{3} [4d_d - d_u]; \quad (32)$$

The analysis of d_n above is at the electro-weak scale and it must be evolved down to the hadronic scale via renormalization group evolution to give

$$d_n^E = {}^E d_n \quad (33)$$

where E is the QCD correction factor and we estimate it to be 1.53 in agreement with the analysis of ref. [10]

4 The Chromoelectric and the CP Violating Purely Gluonic Dimension Six Operators

The quark chromoelectric dipole moment is defined to be the factor d^C in the effective operator

$$L_I = \frac{i}{2} d^C \bar{q} \gamma_5 T^a q G^a \quad (34)$$

where T^a are the generators of SU(3). The gluonic dipole moment d^G is defined to be the factor in the effective operator

$$L_I = \frac{1}{6} d^G f^{abc} G^a G^b G^c \quad (35)$$

where G is the gluon field strength tensor, f are the Gell-Mann coefficients, and ϵ^{0123} is the totally antisymmetric tensor with $\epsilon^{0123} = +1$. An analysis of these operators in minimal supergravity with two CP violating phases was given in ref.[12]. We quote the results from that work here. For the chromoelectric dipole moment one has three contributions; from the gluino exchange, from the neutralino exchange, and from the chargino exchange. These are given by [12]

$$d_{q \text{ gluino}}^C = \frac{g_s}{4} \sum_{k=1}^3 \text{Im} \left(\frac{1}{q} \right) \frac{m_g}{M_{\tilde{q}k}^2} C \left(\frac{m_g^2}{M_{\tilde{q}k}^2} \right); \quad (36)$$

where

$$C(x) = \frac{1}{6(x-1)^2} (10x - 26 + \frac{2x \ln x}{1-x} - \frac{18 \ln x}{1-x}); \quad (37)$$

$$d_{q \text{ neutralino}}^C = \frac{g_s g^2}{16} \sum_{k=1}^3 \sum_{i=1}^4 \text{Im} \left(\frac{m_0}{q_{ik}} \right) \frac{m_{\tilde{q}k}^2}{M_{\tilde{q}k}^2} B \left(\frac{m_{\tilde{q}k}^2}{M_{\tilde{q}k}^2} \right); \quad (38)$$

and

$$d_{q \text{ chargino}}^C = \frac{g_s^2}{16} \sum_{k=1}^3 \sum_{i=1}^2 \text{Im} \left(\frac{m_{\tilde{q}k}}{q_{ik}} \right) \frac{m_{\tilde{q}k}^2}{M_{\tilde{q}k}^2} B \left(\frac{m_{\tilde{q}k}^2}{M_{\tilde{q}k}^2} \right); \quad (39)$$

The contribution to the EDM of the quarks can be computed using the naive dimensional analysis [16] which gives

$$d_q^C = \frac{e}{4} d_q^{C \text{ } ^C} \quad (40)$$

where C is the QCD correction factor for the color dipole operator.

For the CP violating dimension six operator

$$d^G = -3 \sum_t m_t \left(\frac{g_s}{4} \right)^3 \text{Im} \left(\frac{1}{t} \right) \frac{Z_1}{m_g^3} H(Z_1; Z_2; Z_t) \quad (41)$$

where

$$Z_1 = \left(\frac{M_t}{m_g} \right)^2; Z_t = \left(\frac{m_t}{m_g} \right)^2 \quad (42)$$

The contribution to d_n from d^G can be estimated by the naive dimensional analysis [16] which gives

$$d_n^G = \frac{eM}{4} d^{G \text{ } ^G} \quad (43)$$

where M is the chiral symmetry breaking scale and has the numerical value 1.19 GeV, and G is the renormalization group evolution factor of the dimension six operator from the electroweak scale down to the hadronic scale. We estimate that $^G \approx 3.4$ in agreement with the analysis of ref. [10]. To get the contributions

of the chromoelectric and dimension six operators to EDM we used the reduced coupling constant and the naive dimensional analysis. There is another way of estimating this contribution for the chromoelectric operator and that is using QCD sum rules [17]. The use of QCD sum rules rather than of the naive dimensional method would not change the conclusions of this paper.

5 EDM Analysis

As already stated while the EDM of the neutron has been analysed in many works, most of the previous analyses have been carried out within MSSM. Our analysis here is in the framework of $N=1$ supergravity and we use radiative breaking of the electro-weak symmetry including one loop effective potential terms [15] to analyse the EDMs in the six dimensional parameter space of the theory given by $m_0; m_{\frac{1}{2}}; A_0; \tan \beta; \mu$ and α_0 . The constraints imposed on the radiative electro-weak symmetry breaking include imposition of color and charge conservation, experimental lower limit constraints on the sparticle masses from LEP, CDF and D0, and the experimental constraints on $b \rightarrow s + \gamma$ from CLEO [18]. (Details of the analysis are similar to those of Ref. [19]). As mentioned in Sec.1 in most of the previous analyses in the literature the effects of the chromo-electric and of the purely gluonic operators have been assumed small and ignored. As shown in ref. [12] this is an erroneous assumption as the relative contributions of the electric, of the chromo-electric, and of the purely gluonic operators are highly model dependent and their ratios can sharply change as one moves in the six dimensional parameter space of the model. In fact, it was shown in ref. [12] that contrary to the assumptions generally made the contributions of the chromoelectric and of the purely gluonic operators can be comparable to and may even exceed the contribution of the electric dipole term. Because of the significant contribution that the chromo-electric and the purely gluonic operators can make to the neutron EDM we include in our analysis all the three contributions, i.e., the electric, the chromo-electric and the purely gluonic operator contributions. However, we do not include in the analysis the effects induced by the phase in the Kobayashi-Maskawa (KM) mass matrix in the renormalization group evolution of the SUSY phases, since these induced effects are known to be very small [20, 21, 22].

One of the important phenomenon we find in our analysis is the possibility of destructive interference between the gluino and the chargino exchange diagrams for the electric dipole and for the chromoelectric terms. This generally happens

when the signs of phases of ϕ_0 and ϕ_{A0} are opposite. In this case there is also a destructive interference between the ϕ_0 and the A_t terms in the purely gluonic part. In addition to the above one also finds a further cancellation among the electric, the chromoelectric and the purely gluonic parts. Constraints on the theoretical analyses are provided by the experimental upper limits on the EDMs. For the neutron the current experimental limit is [1]

$$d_n < 1.1 \cdot 10^{-25} \text{ ecm} \quad (44)$$

and for the electron the limit is [8]

$$d_e < 4.3 \cdot 10^{-27} \text{ ecm} \quad (45)$$

For the muon the current experimental upper limit is $d_\mu < 1.1 \cdot 10^{-18} \text{ ecm}$ [23] (at 95% C.L.). This limit may improve by up to four orders of magnitude in a new proposed experiment at the Brookhaven National Laboratory [24]. However, the constraints on the supergravity parameter space from the current limits on the neutron EDM and on the electron EDM are already much stronger than what might emerge from the improved muon EDM experiment. For this reason we focus in our analysis on the constraints coming from the neutron EDM and from the electron EDM. However, we shall sometimes also display the muon EDM for comparison along with the neutron and the electron EDM.

We begin our discussion with a comparison between the electron and neutron EDM constraints on the two basic parameters of the theory, i.e., m_0 and $m_{1=2}$. As may be seen from Fig.(2a) the electron EDM falls off with increasing m_0 . This behavior is easily understood from Eqs.(22) and (29) since as m_0 increases $A(r)=M_f^2$ and $B(r)=M_f^2$ decrease. Using the experimental upper limit of Eq.(45) in Fig.(2a) one finds for $\beta_{A0}=1.0$, $\tan\beta=3.0$ and $\phi_0=\phi_{A0}=\frac{\pi}{10}$ the following constraints on m_0 : $m_0 > 1320 \text{ GeV}$ for $m_{1=2} = 700 \text{ GeV}$, $m_0 > 1420 \text{ GeV}$ for $m_{1=2} = 600 \text{ GeV}$, and $m_0 > 1520 \text{ GeV}$ for $m_{1=2} = 500 \text{ GeV}$. A similar analysis holds for Fig.(2b). Here using the experimental upper limit on the neutron EDM of Eq.(44) and for the same above parameters one finds: $m_0 > 2500 \text{ GeV}$ for $m_{1=2} = 700 \text{ GeV}$, $m_0 > 2680 \text{ GeV}$ for $m_{1=2} = 600 \text{ GeV}$ and $m_0 > 2840 \text{ GeV}$ for $m_{1=2} = 500 \text{ GeV}$. Thus in this region of the parameter space the upper limit on the neutron EDM rather than the upper limit on the electron EDM is the more severe constraint on m_0 . The dependence of d_e and d_n on $m_{1=2}$ is displayed in Figs.(2c) and (2d). The broad maxima for small $m_{\frac{1}{2}}$ in these graphs arise from an interplay between the

factors $m_{\frac{1}{2}} + m_{\frac{0}{2}}$ and m_g which increase as $m_{\frac{1}{2}}$ increases, and the functions $A(r)$, $B(r)$ and $C(r)$ which decrease as $m_{\frac{1}{2}}$ increases. By carrying out the same analysis as for the m_0 dependence, one finds here also that the experimental upper limit constraint for the neutron EDM is a more severe constraint than the one for the electron EDM.

The dependence of the EDMs on β_0 is displayed in Fig.(2e) and on $\tan \beta$ in Fig.(2f). The conventional fine tuning problem can be understood from the analysis of Fig.(2e) where the phase β_0 must lie in a very small corridor around the origin to satisfy the current experimental constraints on the neutron EDM. Fig.(2f) shows that the EDMs are an increasing function of $\tan \beta$. This behavior can be understood easily for the electron and for the muon EDM since these involve a factor of $1 = \cos \theta$ which increases as $\tan \beta$ increases. For the neutron EDM case, there are contributions from both the up quark and from the down quark with different $\tan \beta$ dependences. However, the down quark contribution dominates and as Fig.(2f) shows the neutron EDM is still an increasing function of $\tan \beta$.

In the analysis thus far we did not take advantage of the two independent phases. To give a comparison of the results arising in the two cases we consider first the case of Fig.(3a) where the signs of A_0 and β_0 are both positive. Here we find that there are no large internal cancellations within the various components, d_n^E , d_n^C , and d_n^G so these functions do not show any rapidly varying behavior. However, d_n^E and d_n^C in this case are negative while d_n^G is positive over the entire $|\beta_0|$ region and there is a cancellation among them. In the region of $|\beta_0| < 2.5$ the cancellation is rather small because d_n^G is relatively small. However, the cancellation becomes more significant for $|\beta_0| > 2.5$ leading to a dip in the total d_n in this region as seen in Fig.(3a).

We consider next the case in Fig.(3b) when the sign of A_0 is switched. Here each of the individual components d_n^E , d_n^C , and d_n^G shows a destructive interference giving rise to sharp minima as a function of $|\beta_0|$. These minima can be understood as follows: For the case of d_n^E and d_n^C the minima arise as a consequence of destructive interference between the gluino exchange and the chargino exchange in the one loop diagrams. This illustrates what we have said previously that the chargino exchange contributions are as important as the gluino exchange contributions and should be included in the analysis contrary to what is often done in the literature. The minimum in d_n^G in Fig.(3b) has a different origin. It can be understood by

examining the expression

$$\text{Im} \left(\frac{1}{t} \right) = \frac{m_t}{(M_{t1}^2 - M_{t2}^2)} (m_0 \tilde{A}_t j \sin \theta_t + j j \sin \theta_t \cot \theta_t); \quad (46)$$

where θ_t and θ_t are the values of θ_0 and of θ_{A_t} at the electro-weak scale. From Eq.(46) we see that the magnitude of $\text{Im} \left(\frac{1}{t} \right)$ depends on the relative sign and the relative magnitudes of θ_0 and of θ_t . Thus a cancellation occurs between the A_t and the j term when θ_0 and θ_t have opposite signs leading to a sharp minimum in d_n^G as a function of $\tilde{A}_0 j$. Now each of the three terms d_n^E , d_n^C , and d_n^G , switch sign as they pass their zero values. Thus d_n^E and d_n^C are negative below their respective minima and become positive after crossing them, while d_n^G is positive below the minimum and becomes negative after crossing it. This complex structure now gives rise to two distinct minima in the algebraic sum of the three terms, i.e., in the total d_n as may be seen in Fig.(3b). We pause here to note that for the case when there is destructive interference between the gluino and the chargino case, and a further cancellation among the electric, the chromoelectric and the purely gluonic terms as is the case for Fig.(3b), one finds a drastic reduction in the magnitude of d_n often by a factor $O(10^{-3})$.

In Fig.(3c) we give a plot of the EDMs of the electron, the muon and the neutron as a function of $m_{1=2}$ showing the cases when A_0 is positive and when A_0 is negative. Here for the case when A_0 is positive the neutron EDM is large enough that it violates the current experimental bound in the entire range of $m_{1=2} = 750$ GeV. However, for the case when A_0 is negative the neutron EDM lies below the experimental upper limit for $m_{1=2} = 300$ GeV. The large disparity between the magnitudes of the neutron EDM for the A_0 positive case vs for the A_0 negative case can shift the balance between which of the two experimental constraints, i.e., the experimental upper limit constraint on the neutron EDM or the experimental upper limit constraint on the electron EDM, is the more stringent one. It can be seen that for the case of constructive interference the experimental upper limit constraint on the neutron EDM is generally the more stringent one while for the case of destructive interference involving large cancellation it is the experimental constraint on the electron EDM which may be the more stringent constraint. We shall exhibit this effect further in the analysis of Fig.(3e).

The destructive interference between the different contributions exhibited in Figs. (3a) – (3c) is not an isolated phenomenon but rather a common occurrence in a large part of the parameter space. Thus, cancellations occur naturally over

the entire parameter space with the appropriate choice for the relative sign of μ and A_0 . Further, these cancellations can become exceptionally large in certain regions of the parameter space. An example of this effect already occurs in the analysis of Figs.(3b) and (3c). Similar cancellations also appear in other regions of the parameter space. In Fig.(3d) the effect of cancellations in d_n is shown as a function of m_0 for three sets of input data for the case when μ and A_0 have opposite signs. In each case there are large cancellations which lead to the appearance of minima. Aside from the reduction of the EDMs by cancellations, there are regions of the parameter space where kinematical suppressions occur. An example of this is the reduction of the EDMs when $\tan\beta$ becomes small as may be seen in Fig.(2f). A kinematical suppression of the EDMs can also occur if $m_{\frac{1}{2}}=m_0 \ll 1$. As one can see from Eqs.(19) and (29) that in this case the quark and the lepton EDMs are kinematically suppressed. A suppression of this type appears to arise in supersymmetric models with anomalous U(1) mediated supersymmetry breaking [25].

Finally, we exhibit in Fig.(3e) the excluded regions in the m_0 - $m_{1=2}$ plane under the constraints given by the current experimental upper limits on d_e and d_n . The regions between the axes and the curves are the excluded regions in Fig.(3e). The analysis of Fig.(3e) shows the dramatic effect of the destructive interference on the allowed and the disallowed region in the mass plot. One finds that destructive interference softens significantly the stringent constraints on m_0 and $m_{1=2}$. Thus the excluded region in the m_0 - $m_{1=2}$ plane for the destructive interference case is much smaller than for the constructive interference case. The analysis of Fig.(3e) illustrates another interesting phenomenon alluded to earlier. One finds from Fig.(3e) that for the constructive interference case the d_n experimental constraint is the more severe one as it eliminates a larger part of the parameter space, while for the destructive interference case the d_e experimental constraint is the more severe one as it excludes a larger part of the parameter space in the m_0 - $m_{1=2}$ plane in this case.

In the above we have discussed cancellations which can result in a drastic reduction for the case of the neutron edm. There can also be cancellations for the case of the electron edm between the chargino and the neutralino contributions. For comparable sizes of μ and A_0 , the chargino contribution is much larger than the neutralino contribution and cancellation is not very effective. However, more significant cancellations can occur for very small values of μ and for moderate

values of A_0 since in this case the contribution from the chargino exchange and the neutralino exchange become comparable.

6 Conclusion

In this paper we have presented an analysis of the EDM of the neutron and of the charged leptons within the framework of supergravity grand unification under the constraint of radiative breaking of the electroweak symmetry. All the supersymmetric one-loop contributions to the EDMs were analyzed taking care of their relative signs. For the neutron we considered also the contributions from the chromoelectric and from the purely gluonic operators. One finds that there exist significant regions of the parameter space where cancellations occur among the different contributions for the case of the neutron electric dipole moment. In these regions the neutron EDM undergoes a significant reduction and the current experimental limits are consistent in these regions with CP violating phases which are not too small and with a SUSY mass spectrum which satisfies the naturalness constraint. One also finds that regions of the parameter space exist where the destructive interference between the different components can reduce the magnitude of the neutron EDM even below the magnitude of the electron EDM.

The nature of interference, i.e., constructive vs destructive, for the neutron EDM determines which of the two experimental upper limit constraints, i.e., the upper limit on the neutron EDM, or the upper limit on the electron EDM, will constitute the more stringent constraint. For the case of constructive interference for d_n , it is the experimental upper limit on d_n itself which is found to be generally more stringent constraint than the upper limit constraint on d_e . However, for the destructive interference case for d_n , one finds that it is generally the upper limit constraint on d_e which becomes the more stringent constraint.

As mentioned already the previously known mechanisms for the suppression of the neutron EDM in SUSY theories consist of suppression either by a fine tuning using small phases or by a choice of a heavy SUSY spectrum. We have pointed out a third possibility, i.e., that of internal cancellations, which naturally suppress the neutron EDM without the necessity of either having very small phases or having an excessively heavy SUSY spectrum. The cancellations that occur do not constitute a fine tuning. Rather, one finds that such cancellations occur naturally over a large part of the parameter space, and in some regions the cancellations become exceptionally large. This result has important implications for the discovery of

supersymmetric particles. With the cancellation mechanism the SUSY spectrum within the current naturalness limits can be consistent with the present EDM experimental constraints without the retuning of phases, and such a spectrum should still be within reach of the LHC. At the same time one also expects that if SUSY phases are indeed $O(1 \cdot 10^{-1})$ and the SUSY spectrum lies in the usual naturalness limit of $O(1)$ TeV, then with the suppression of the neutron EDM via the cancellation mechanism the neutron and the electron EDMs should become visible with improvements of $O(10)$ in the sensitivity of the EDM experiments. Finally we point out that although our analysis has been done in the framework of supergravity unification with soft SUSY breaking sector parametrized by six parameters (including two CP violating phases), the mechanism of internal cancellations pointed out in this paper which can suppress the EDMs should be applicable to a wider class of models such as models with non-universal soft SUSY breaking.

7 Acknowledgements

This research was supported in part by NSF grant PHY-96020274.

8 Appendix A

The squark (mass)² matrix

$$M_{\tilde{q}}^2 = \begin{pmatrix} M_{\tilde{q}11}^2 & M_{\tilde{q}12}^2 \\ M_{\tilde{q}21}^2 & M_{\tilde{q}22}^2 \end{pmatrix}; \quad (47)$$

is hermitian and can be diagonalized by the unitary transformation

$$D_{\tilde{q}}^\dagger M_{\tilde{q}}^2 D_{\tilde{q}} = \text{diag}(M_{\tilde{q}1}^2, M_{\tilde{q}2}^2) \quad (48)$$

where one parametrizes $D_{\tilde{q}}$ so that

$$D_{\tilde{q}} = \begin{pmatrix} \cos \frac{\varphi}{2} & \sin \frac{\varphi}{2} e^{i\varphi} \\ \sin \frac{\varphi}{2} e^{i\varphi} & \cos \frac{\varphi}{2} \end{pmatrix}; \quad (49)$$

Here $M_{\tilde{q}21}^2 = M_{\tilde{q}21}^2 e^{i\varphi}$ and we choose the range of φ so that $-\frac{\pi}{2} < \varphi < \frac{\pi}{2}$ where $\tan \varphi = \frac{2M_{\tilde{q}21}^2}{M_{\tilde{q}11}^2 - M_{\tilde{q}22}^2}$. The eigenvalues $M_{\tilde{q}1}^2$ and $M_{\tilde{q}2}^2$ can be determined directly from Eq.(48) or from the roots

$$M_{\tilde{q}(1)(2)}^2 = \frac{1}{2} (M_{\tilde{q}11}^2 + M_{\tilde{q}22}^2) (\pm) \left(\right) \frac{1}{2} [(M_{\tilde{q}11}^2 - M_{\tilde{q}22}^2)^2 + 4M_{\tilde{q}21}^2]^{\frac{1}{2}}; \quad (50)$$

The (+) in Eq.(50) corresponds to choosing the structure of the matrix M_q^2 so that for $M_{q11}^2 > M_{q22}^2$ one has $M_{q1}^2 > M_{q2}^2$ and vice versa. For our choice of the θ_q range one has

$$\tan \theta_q = \frac{2m_q \tilde{A}_q m_0}{M_{q11}^2 - M_{q22}^2} R_q j \quad (51)$$

where $R_u = \cot \theta_u$ and $R_d = \tan \theta_d$. Further

$$\sin \theta_q = \frac{m_0 \tilde{A}_q j \sin \theta_q + j j \sin \theta_q}{j n_0 A_q R_q j} : \quad (52)$$

Using the above we get

$$\text{Im}(\theta_q^{11}) = \text{Im}(\theta_q^{12}) = \frac{1}{2} \sin \theta_q \sin \theta_q \quad (53)$$

where

$$\sin \theta_q = \frac{2m_q \tilde{A}_q m_0}{M_{q1}^2 - M_{q2}^2} R_q j \quad (54)$$

the θ_q in Eq.(54) depends on whether $M_{q11}^2 - M_{q22}^2$ is $> 0 (< 0)$. Thus Eq.(53) gives

$$\text{Im}(\theta_q^{11}) = \frac{m_q}{M_{q1}^2 - M_{q2}^2} (m_0 \tilde{A}_q j \sin \theta_q + j j \sin \theta_q); \quad (55)$$

which holds quite generally, i.e., for the case where $M_{q1}^2 > M_{q2}^2$ and for the case where $M_{q1}^2 < M_{q2}^2$. Thus the gluino contribution to the EDM of the quark is given by

$$d_{q \text{ gluino}}^E = e = \frac{2}{3} s_m Q_q \text{Im}(\theta_q^{11}) \left[\frac{1}{M_{q1}^2} B\left(\frac{m_g^2}{M_{q1}^2}\right) - \frac{1}{M_{q2}^2} B\left(\frac{m_g^2}{M_{q2}^2}\right) \right]; \quad (56)$$

One may expand the right hand side of Eq.(56) around the average squark mass. Defining $M_q^2 = (M_{q1}^2 + M_{q2}^2)/2$, and expanding in the difference $(M_{q1}^2 - M_{q2}^2)$, one finds in the lowest approximation

$$d_{q \text{ gluino}}^E = e' \frac{2}{3} s_m Q_q \frac{m_q}{M_q^4} (m_0 \tilde{A}_q j \sin \theta_q + j j \sin \theta_q) \left(B\left(\frac{m_g^2}{M_q^2}\right) + \frac{m_g^2}{M_q^2} D\left(\frac{m_g^2}{M_q^2}\right) \right) \quad (57)$$

where $D(r)$ is given by

$$D(r) = \frac{1}{2(1-r)^3} (5 + r + 2 \ln r + \frac{6r \ln r}{(1-r)}); \quad (58)$$

As mentioned already currently there is some confusion in the literature regarding the sign of the gluino contribution to the electric dipole operator [6, 7]. We first compare our results with those of ref. [7]. The analysis of [7] corresponds to neglecting the D term in Eq.(57) and using $d_n = \frac{4}{3}d_d$ which gives

$$\frac{d_n}{e} = \frac{8}{27} m_g m_d \left[\frac{m_0 A_d j \sin \alpha_d + j j \sin \alpha_d \tan \beta}{M_{\tilde{g}}^4} \right] \left(\frac{m_g^2}{M_{\tilde{g}}^2} \right) \quad (59)$$

This result then agrees both in sign and in magnitude with Eq.(3) of ref. [7]. To compare with the result of ref. [6] we switch the sign of the m_H term in their Eq.(6) (see e.g., ref. [26]) and find that our Eq.(19) differs from Eq.(14) of ref. [6] by an overall minus sign. A comparison of the chargino and the neutralino contributions with those of ref. [6] is more involved since the chargino (and the neutralino) mass matrices are different in the two works. This difference arises because after $SU(2)_L \times U(1)_Y$ breaking to $U(1)_{EM}$, the authors of ref. [6] expand the potential around the VEV so that $H_i = H_i + h H_i$ instead of $H_i = H_i + h H_i$ and they use in the chargino case M_C^T instead of M_C as is conventionally done [26]. Thus to compare with their expressions we have to do the transformation: $V_{ij} = C_{Rji}$, $U_{ij} = C_{Lji}$, $D = S$ and $X = N$. After that, and assuming the conventional expansion around the VEV, we go to their convention by the transformation $\tilde{f} = \tilde{f}$ to find that we have the same overall sign in the case of the chargino exchange but the sign of the \tilde{f}^0 term in the brackets in their Eq.(10) should be positive. In the case of neutralino exchange our result differs from their Eq.(12) by an overall sign and further we find that the second term in the last bracket of their Eq.(13) (the term which begins with $-\tilde{f}$) should have an opposite sign.

9 Appendix B

The chargino matrix M_C is not hermitian, not symmetric and not real because is complex. M_C is diagonalized using the biunitary transformation

$$U^0 M_C V^{-1} = M_D \quad (60)$$

where U^0 and V are hermitian and M_D is a diagonal matrix but not yet real. U^0 and V satisfy the relation

$$V (M_C^Y M_C) V^{-1} = \text{diag}(j\tilde{f}_1 + \tilde{f}_1^2; j\tilde{f}_2 + \tilde{f}_2^2) = U^0 (M_C M_C^Y) (U^0)^{-1} \quad (61)$$

We may parametrize U^0 so that

$$U^0 = \begin{pmatrix} \cos \frac{1}{2} & \sin \frac{1}{2} e^{i_1} \\ \sin \frac{1}{2} e^{-i_1} & \cos \frac{1}{2} \end{pmatrix}; \quad (62)$$

where

$$\tan \frac{1}{2} = \frac{2^{1/2} \bar{m}_W [\bar{m}_2^2 \cos^2 + j j^2 \sin^2 + j j \bar{m}_2 \sin 2 \cos]^{1/2}}{\bar{m}_2^2 - j j^2 - 2 \bar{m}_W^2 \cos 2} \quad (63)$$

and

$$\tan \frac{1}{2} = \frac{j j \sin \frac{1}{2}}{\bar{m}_2 \cos \frac{1}{2} + j j \cos \frac{1}{2} \sin \frac{1}{2}} \quad (64)$$

Similarly we parametrize V so that

$$V = \begin{pmatrix} \cos \frac{2}{2} & \sin \frac{2}{2} e^{i_2} \\ \sin \frac{2}{2} e^{-i_2} & \cos \frac{2}{2} \end{pmatrix}; \quad (65)$$

where

$$\tan \frac{2}{2} = \frac{2^{1/2} \bar{m}_W [\bar{m}_2^2 \sin^2 + j j^2 \cos^2 + j j \bar{m}_2 \sin 2 \cos]^{1/2}}{\bar{m}_2^2 - j j^2 + 2 \bar{m}_W^2 \cos 2} \quad (66)$$

and

$$\tan \frac{2}{2} = \frac{j j \sin \frac{2}{2}}{\bar{m}_2 \sin \frac{2}{2} + j j \cos \frac{2}{2} \cos \frac{2}{2}}; \quad (67)$$

We wish to choose the phases of U^0 and V so that the elements of M_D will be positive. Thus we define $U = H U^0$ where

$$H = \begin{pmatrix} e^{i_1} & 0 \\ 0 & e^{i_2} \end{pmatrix}; \quad (68)$$

such that

$$U M_C V^{-1} = \begin{pmatrix} j \bar{m}_1 + j & 0 \\ 0 & j \bar{m}_2 + j \end{pmatrix}; \quad (69)$$

where \bar{m}_1 and \bar{m}_2 are the phases of the diagonal elements in Eq.(60). Our choice of the signs and the roots is such that

$$\begin{aligned} M_{(\bar{m}_1 + j)(\bar{m}_2 + j)}^2 &= \frac{1}{2} [\bar{m}_2^2 + j j^2 + 2 \bar{m}_W^2] (+)(-) \\ &= \frac{1}{2} [(\bar{m}_2^2 - j j^2)^2 + 4 \bar{m}_W^4 \cos^2 2 + 4 \bar{m}_W^2 \\ &\quad (\bar{m}_2^2 + j j^2 + 2 \bar{m}_2 j j \cos \frac{1}{2} \sin 2)]^{1/2} \end{aligned} \quad (70)$$

where the sign chosen is such that $\bar{m}_1 + j < \bar{m}_2 + j$ if

$$\bar{m}_2^2 < j j^2 + 2 \bar{m}_W^2 \cos 2; \quad (71)$$

For the neutralino matrix, the eigenvalues and the diagonalizing matrix X must be estimated numerically.

References

- [1] I.S. Altarev et al., Phys. Lett. B 276, 242 (1992); K.F. Smith et al., Phys. Lett. B 234, 191 (1990); N.F. Ramsey, Annu. Rev. Nucl. Part. Sci. 40, 1 (1990)
- [2] J. Ellis, S. Ferrara and D.V. Nanopoulos, Phys. Lett. B 114, 231 (1982); W. Buchmüller and D. Wyler, Phys. Lett. B 121, 321 (1983); F. del'Aguila et al., Phys. Lett. B 126, 71 (1983); J. Polchinski and M.B. Wise, Phys. Lett. B 125, 393 (1983); J.-M. Gerard et al., Nucl. Phys. B 253, 93 (1985); E. Franco and M. Mangano, Phys. Lett. B 135, 445 (1984);
- [3] M. Dugan, B. Grinstein and L. Hall, Nucl. Phys. B 255, 413 (1985); A. Sanda, Phys. Rev. D 32, 2292 (1985); T. Kurokawa, Prog. Theor. Phys. 73, 209 (1985).
- [4] For a recent review see, S.M. Barr and W.J. Marciano, in "CP Violation", ed. C. Jarlskog, (1989, World Scientific, Singapore), p. 455; W. Bernreuther and M. Suzuki, Rev. Mod. Phys. 63, 313 (1991).
- [5] P. Nath, Phys. Rev. Lett. 66, 2565 (1991).
- [6] Y. Kizukuri and N. Oshimo, Phys. Rev. D 46, 3025 (1992); *ibid.* D 45, 1806 (1992).
- [7] R. Garisto, Nucl. Phys. B 419, 279 (1994).
- [8] E. Commins, et. al., Phys. Rev. A 50, 2960 (1994); K. Abdullah, et. al., Phys. Rev. Lett. 65, 234 (1990).
- [9] S. Weinberg, Phys. Rev. Lett. 63, 2333 (1989); E. Braaten, C.S. Li, and T.C. Yuan, *ibid.*, 64, 1709 (1990); J. Dai, H. Dykstra, R.G. Leigh, S. Paban, and D.A. Dicus, Phys. Lett. B 237, 216 (1990).
- [10] R. Amswitt, J. Lopez and D.V. Nanopoulos, Phys. Rev. D 42, 2423 (1990); R. Amswitt, M. Du and K. Stelle, Phys. Rev. D 43, 3085 (1991).
- [11] T. Falk, K.A. Olive, and M. Srednicki, Phys. Lett. B 354, 99 (1995); T. Falk and K.A. Olive, Phys. Lett. B 375, 196 (1996).
- [12] T. Ibrahim and P. Nath, hep-ph/9707409 (To appear in Physics Letters B).
- [13] A. Chamseddine, R. Amswitt and P. Nath, Phys. Rev. Lett. 49, 970 (1982).

- [14] P. Nath, R. A mow itt and A H. Cham seddine, Applied N=1 supergravity, Lecture series,1983 (W orld Scienti c, Singapore); H .P.N illes, Phys.Rep.110, 1 (1984); H E .H aber, G L Kane. Phys.Rep.117, 195 (1985). H E .H aber, TASI Lecture, SC IPP 92/33 (1992).
- [15] S. Coleman and E. Weinberg, Phys. Rev. D 7, 1888 (1973); J Ellis, G. Rido and F. Zwimer, Phys. Lett. B 262, 477 (1991); R. A mow itt and P. Nath, Phys. Rev. D 46, 3981 (1992).
- [16] A. M anohar and H. Georgi, Nucl. Phys. B 234, 189 (1984).
- [17] I B. K hriplovich and K N. Zyablyuk, Phys. Lett. B 383, 429 (1996).
- [18] R. Am m ar et. al. (CLEO Collaboration), Phys. Rev. Lett. 71, 674 (1993).
- [19] R. A mow itt and P. Nath, Phys. Rev. Lett. 69, 725 (1992); for a recent review see, R. A mow itt and P. Nath, Lectures at V II Sw ieca Sum m er School, Com pos de Jordao, Brasil (W orld Scienti c, Singapore, 1994).
- [20] T. Inui, Y. M im ura, N. Sakai, and T. Sasaki, Nucl. Phys. B 449 (1995)4.
- [21] C. Ham zaoui, M. Pospelov and R. Roiban. hep-ph/9702292
- [22] S. Bertolini, F. V issani. Phys. Lett. B 324, 164 (1994).
- [23] J. Bailey et. al., Nucl. Phys. B 150, 1 (1979).
- [24] Y. Sem ertzidis et. al., E 821 Collaboration at BNL, Design Report, BNL AG S E 81 (1995).
- [25] G. D vali and A. Pom erol, Phys. Rev. Lett. 77, 3728 (1996); R. N. M ohapatra and A. R iotto, Phys. Rev. D 55, 4262 (1997).
- [26] H E .H aber, J F. G union. Nucl. Phys. B 272, 1 (1986); E : Nucl. Phys. B 402, 567 (1993).

Figure Captions

Fig. (1a): One loop diagram contributing to the electric dipole operator where the external photon line ends on an exchanged chargino line labelled by $\tilde{\chi}_i^+$ in the loop.

Fig. (1b): One loop diagram contributing to the electric dipole operator where the external photon line ends on an exchanged squark (slepton) line represented by $\tilde{q} (\tilde{l})$ on the internal line.

Fig. (2a): Plot of the magnitude of the electron EDM as a function of m_0 when $\tilde{A}_0 = 1.0$, $\tan \beta = 3.0$ and $\mu = \frac{m_0}{10}$ for different values of $m_{1=2}$. The dotted curve is for $m_{1=2} = 500$ GeV, the solid curve for $m_{1=2} = 600$ GeV, and the dashed curve is for $m_{1=2} = 700$ GeV.

Fig. (2b): Plot of the magnitude of the neutron EDM as a function of m_0 for the same parameters as in Fig. 2 (a).

Fig. (2c): Plot of the magnitude of the electron EDM as a function of $m_{1=2}$ when $\tilde{A}_0 = 1.0$, $\tan \beta = 3.0$ and $\mu = \frac{m_0}{10}$ for different values of m_0 . The dotted curve is for $m_0 = 500$ GeV, the solid curve for $m_0 = 1000$ GeV and the dashed curve is for $m_0 = 1500$ GeV.

Fig. (2d): Plot of the magnitude of the neutron EDM as a function of $m_{1=2}$ for the same parameters as in Fig. 2 (c).

Fig. (2e): Plot of the magnitudes of the neutron, the electron and the muon EDMs as a function of μ for the case when $\tilde{A}_0 = 1.0$, $\tan \beta = 3.0$, $\mu = \frac{m_0}{20}$, $m_0 = 1000$ GeV and $m_{1=2} = 500$ GeV.

Fig. (2f): Plot of the magnitudes of the neutron, the electron and the muon EDMs as a function of $\tan \beta$ for the case when $\tilde{A}_0 = 1.0$, $\mu = \frac{m_0}{20}$, $m_0 = 2000$ GeV and $m_{1=2} = 500$ GeV.

Fig. (3a): Plot of the magnitudes of the electric dipole contribution, of the color dipole contribution, of the purely gluonic contribution, and of the total neutron

EDM as a function of \tilde{A}_0 for the case when $\tan \beta = 3$, $\mu_0 = \frac{1}{30}$, $A_0 = \frac{1}{8}$, $m_g = 800$ GeV ($m_{1=2} = 281.2$ GeV) and $m_0 = 1500$ GeV.

Fig. (3b): Same as Fig.(3a) except that $A_0 = \frac{1}{8}$.

Fig. (3c): Plot of the magnitudes of the neutron, the electron and the muon EDMs as a function of $m_{1=2}$ for the case when $\tan \beta = 3$, $\mu_0 = \frac{1}{30}$, $A_0 = \frac{1}{8}$, $m_0 = 800$ GeV and $\tilde{A}_0 = 2.6$. The curve 1 (dotted) is for the case when $A_0 = \frac{1}{8}$ and curve 2 (solid) is for case when $A_0 = \frac{1}{8}$.

Fig. (3d): Plot of the magnitudes of the neutron EDM as a function of m_0 for three cases when $\mu_0 = \frac{1}{20}$, $A_0 = \frac{1}{6}$, and $\tan \beta = 3$. The data for the other SUSY parameters is as follows: $\tilde{A}_0 = 2.5$, $m_g = 500$ GeV for curve 1, $\tilde{A}_0 = 2.0$, $m_g = 500$ GeV for curve 2, and $\tilde{A}_0 = 2.5$, $m_g = 600$ GeV for curve 3.

Fig. (3e): The excluded regions in the $m_0 - m_{1=2}$ plane of the minimal SUGRA model under the experimental constraints of Eqs.(44) and (45) when $\tilde{A}_0 = 1.4$, $\tan \beta = 3.0$, $\mu_0 = \frac{1}{30}$ and $A_0 = \frac{1}{8}$. The neutron EDM curves are solid with $n(\)$ corresponding to $A_0 = \frac{1}{8}$, and the electron EDM curve is dotted and labelled e(+;). The excluded regions of the parameter space lie between the axes and the curves.

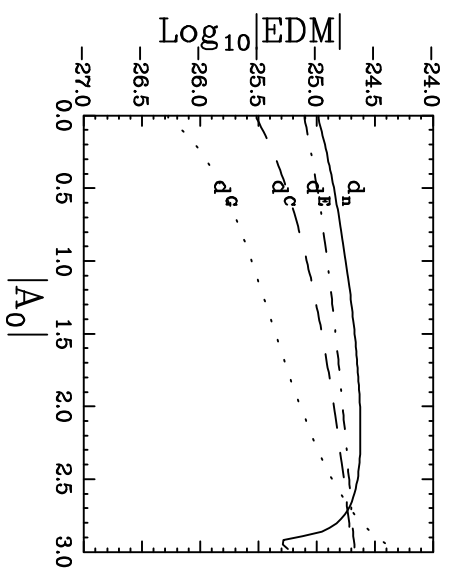


Fig. (3a)

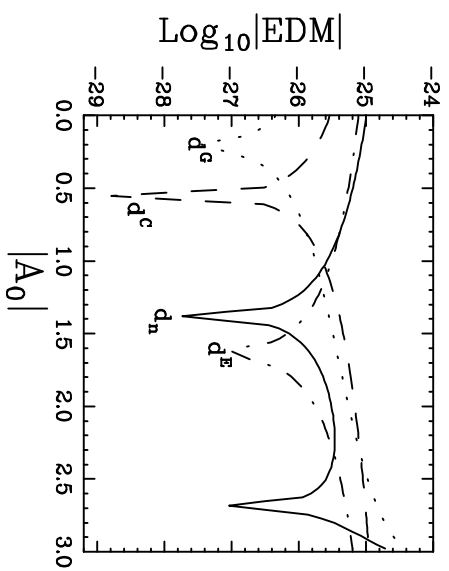


Fig. (3b)

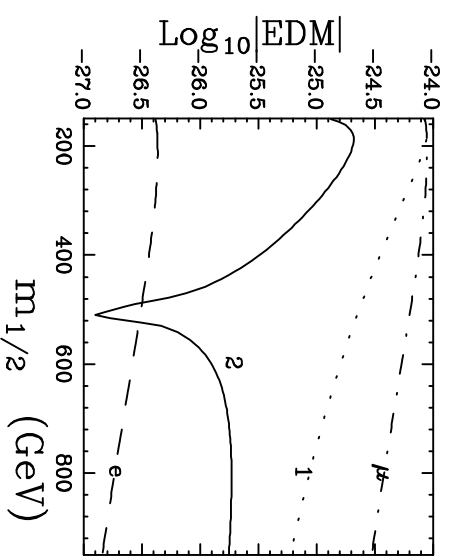


Fig. (3c)

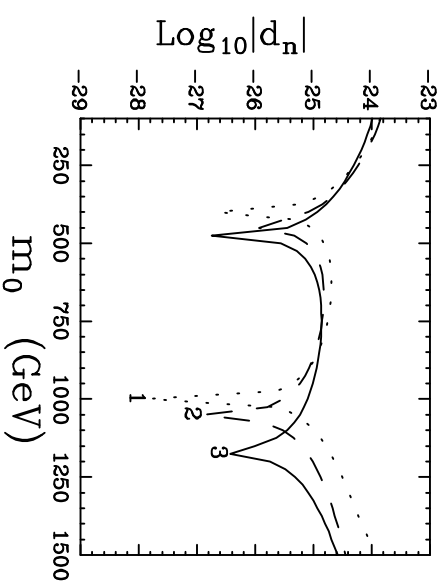


Fig. (3d)

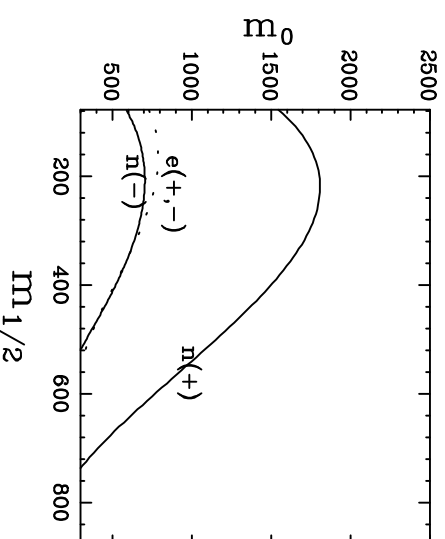


Fig. (3e)

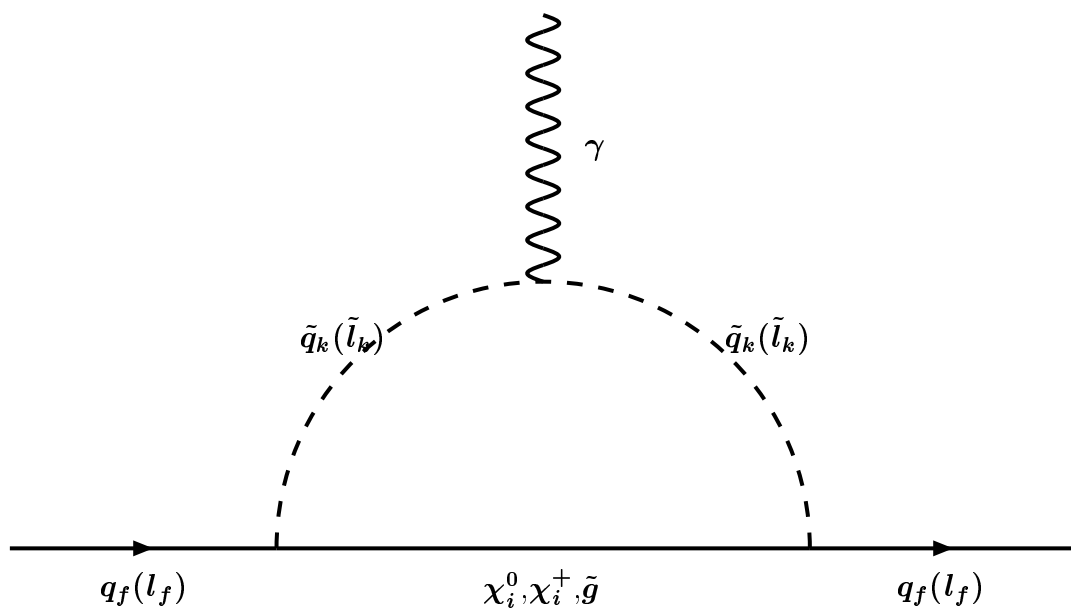


Fig. (1b)

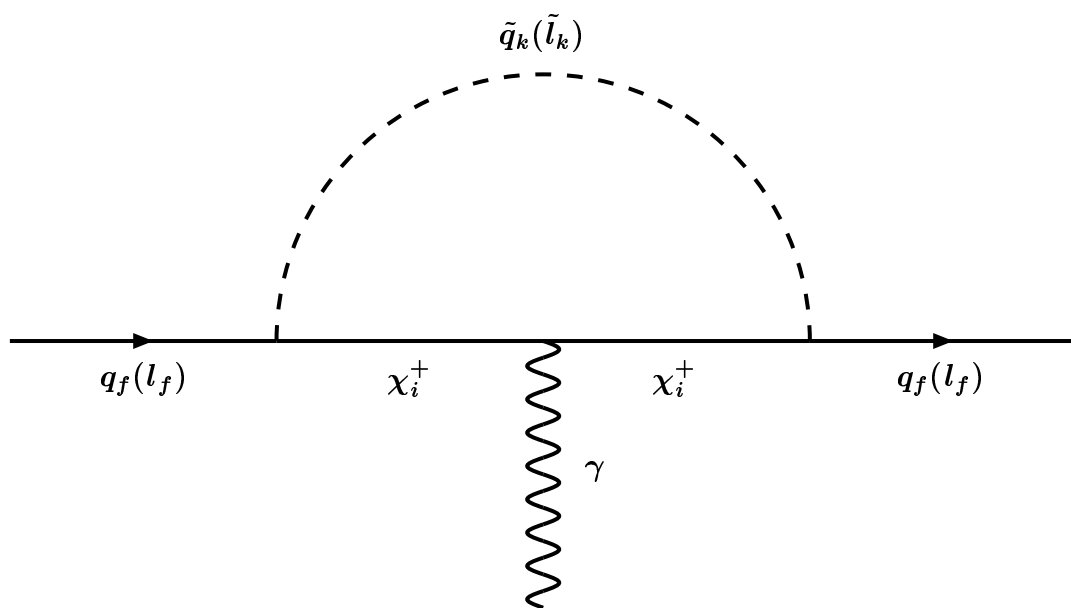


Fig. (1a)

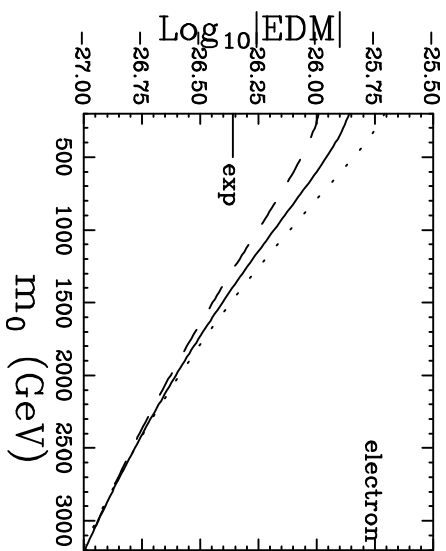


Fig. (2a)

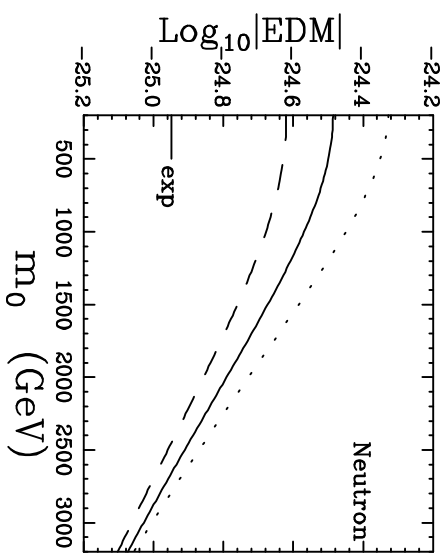


Fig. (2b)

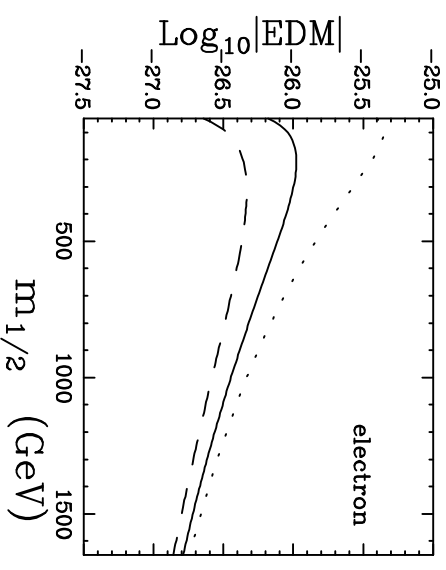


Fig. (2c)

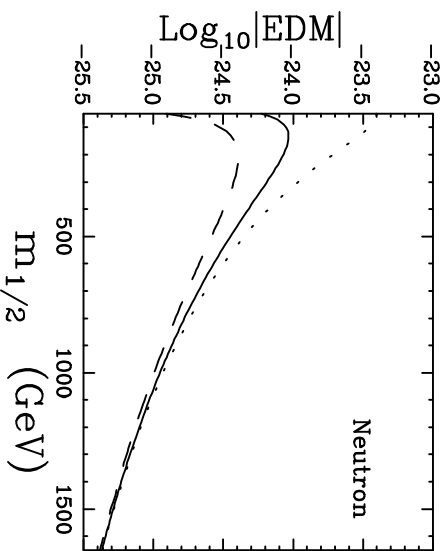


Fig. (2d)

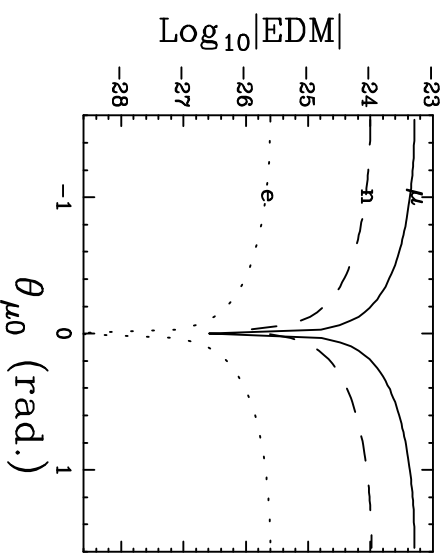


Fig. (2e)

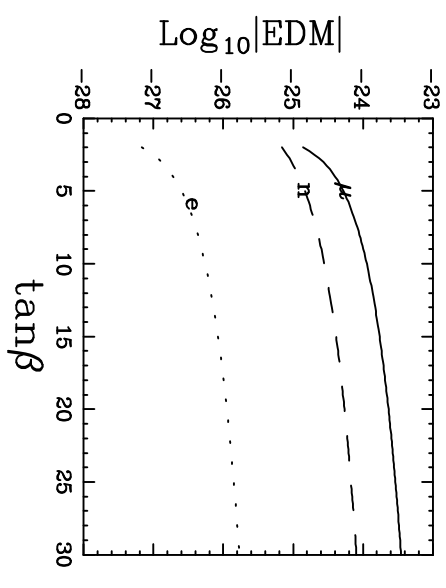


Fig. (2f)